

These studies have concentrated on the ill or zero. The curve $F_0 = 0$ of Figure 2.2.1 is bounded by the ship's wake angle, which is $\sin(1/3) = 19.5^\circ$, spanning the ship's *in ship-wake wedge angle*, and is also bounded by the group velocity vector at the Kelvin angle curve; all other group velocity vectors lie between these two, so that the corresponding waves lie outside the boundary of the wedge have a finite amplitude and the region is an example of a *caustic* with no waves and a region where two waves interfere. The wave field is evanescent outside the wedge angle, which implies that beyond the Kelvin wedge angle (Lightfoot 1978)

produced by boats and ships show that they generate waves with a spectrum of dominant wavenumber $k \sim 2\pi/L$, where L is the length of the ship. For these waves, (2.2.32) gives

$$\left(\frac{2\pi U^2}{gL}\right)^2 - 1\right]^{1/2}. \quad (2.2.33)$$

For a liner or large container vessel, the ship's length L and width m are transverse, behind the ship $U^2/gL \gg 1$, as for a speedboat, (2.2.33) shows that the wake is concentrated in a wedge of angular width much less than the Kelvin angle α_K , and it is similarly small angle to the boat's

wake angle increases and the wake is wider than the wake angle for $F_0 \geq 0.7$. For $F_0 \geq 1$, the wake is narrower than the hydrostatic wake described above close to 90° , but it decreases as F_0 approaches the Kelvin wake angle as $F_0 \rightarrow 3$. When $F_0 > 3$, where the wake is confined to a narrow wake as F_0 increases to values of small craft at high speed with $F_0 \ll 1$, has been incorrectly attributed to shallow water theory in the past. Ship wake situations where the wake is wider than the rule, but are possible in

2.3 One-dimensional non-linear hydrostatic flow

shallow water (for example, $F_0 = 1$ for ship (or boat) speed $U = 28$ knots in water of 20 m depth). For the case of forcing by topography, where U is the current speed, Froude numbers of order unity are common in shallow, fast-moving streams, and the resulting non-linear effects are discussed in the following sections. But for most of the time, for most rivers, the Froude numbers are small. In the stratified analogues to be discussed in subsequent chapters, and which are our primary concern, Froude numbers of all values are possible.

I am not aware of any detailed observational tests of the linear theory for two-dimensional ship wakes, but the latter gives a good qualitative description of the disturbances produced by ducks, boats etc. (Examples are shown in Stoker 1957 and Lighthill 1978.) For flow over topography, there is no reason to question the validity of linear theory for sufficiently small h , but this range of validity is dependent on F_0 .

2.3 One-dimensional non-linear hydrostatic flow

We now return to one-dimensional flow and investigate non-linear effects. These phenomena are most readily appreciated in the hydrostatic system with its long horizontal length-scales, where dispersive effects are not present. From (2.1.6, 2.1.8) we obtain for this system, with $d = d_0 + \eta - h$,

$$u_t + uu_x = -g\eta_x, \quad (2.3.1)$$

$$d_t + (du)_x = 0, \quad (2.3.2)$$

or alternatively

$$\eta_t + [(d_0 + \eta)u]_x = (uh)_x \quad (2.3.3)$$

and we again take the initial conditions (2.2.3), namely $u = U$, $\eta = h$, $\eta_t = 0$, at $t = 0$. This is a classic system of hyperbolic differential equations with a forcing term, which may be expressed in the characteristic form

$$\frac{dx}{dt}(u \pm 2\sqrt{gd}) = -g\frac{dh}{dx}, \quad (2.3.4)$$

on the respective characteristic curves, which are given by

$$\frac{dx}{dt} = u \pm \sqrt{gd}. \quad (2.3.5)$$

(For a discussion of this type of mathematical system, see Whitham 1974; an interesting geometrical approach has been described by Broad

et al. 1993). For small times, the solution of this initial-value problem is essentially the same as for the linear system, and it is given by (2.2.5) and displayed in Figure 2.1. The flow is still governed by the value of the Froude number for the undisturbed flow $F_0 = U/\sqrt{gd_0}$, but as time increases the characteristics over the obstacle do not remain straight but become curved, depending on the values of the flow variables u and d . Representative examples for $F_0 < 1$ and $F_0 > 1$, showing the characteristics of the upstream-propagating waves only, are presented in Figure 2.6. In most situations of interest, the downstream-propagating wave (on the characteristics $dx/dt = u + \sqrt{gd}$) is little affected by non-linearities, and travels quickly downstream away from the vicinity of the obstacle. Whilst necessary to satisfy the initial conditions, these waves are unimportant otherwise and are not relevant to the following discussion. However, on the upstream side of the obstacle, the equations for the variables on this same family of characteristics ((2.3.4, 2.3.5) with the plus sign) may be integrated to yield

$$u + 2\sqrt{gd} = U + 2\sqrt{gd_0}, \quad (2.3.6)$$

since the initial conditions are the same for each member of this family of characteristics on the upstream side. Substituting (2.3.6) into (2.3.4, 2.3.5) then yields, for the other set of characteristics (for waves propagating against the flow),

$$\frac{du}{dt} = \frac{dd}{dt} = 0, \quad \text{on } \frac{dx}{dt} = U + 2\sqrt{gd_0} - 3\sqrt{gd}, \quad (2.3.7)$$

on the upstream side of the obstacle. In this region, d is constant on each characteristic which is therefore straight, but the slopes are different for different characteristics. The result is that, for $F_0 > 1$, the characteristics converge and intersect, as shown in Figure 2.6a, because a disturbance of larger elevation travels faster. For $F_0 > 1$ the effect may be large enough to cause the upstream waves over the obstacle to change direction, as shown in Figure 2.6b. The same processes occur, *mutatis mutandis*, on the downstream side.

This phenomenon of wave speed being dependent on wave amplitude is termed *amplitude dispersion*, and is illustrated in a simpler form in Figure 2.7. A wave of elevation, here simplified to a monotonic increase in surface level moving to the left into undisturbed fluid, is also governed by (2.3.6) and (2.3.7), which show that the interface steepens with time as shown in Figure 2.7a. On the other hand, a decrease in surface level moving in the same direction and leaving

he solution of this initial-value problem is linear system, and it is given by (2.2.5) the flow is still governed by the value of undisturbed flow $F_0 = U/\sqrt{gd_0}$, but as tics over the obstacle do not remain depending on the values of the flow ative examples for $F_0 < 1$ and $F_0 > 1$, the upstream-propagating waves only, most situations of interest, the down- he characteristics $dx/dt = u + \sqrt{gd}$) is s, and travels quickly downstream away e. Whilst necessary to satisfy the initial important otherwise and are not relevant. However, on the upstream side of the he variables on this same family of (with the plus sign) may be integrated to

$$\bar{d} = U + 2\sqrt{gd_0}, \quad (2.3.6)$$

the same for each member of this family am side. Substituting (2.3.6) into (2.3.4), ther set of characteristics (for waves

$$\frac{dx}{dt} = U + 2\sqrt{gd_0} - 3\sqrt{gd}, \quad (2.3.7)$$

ostacle. In this region, d is constant on herefore straight, but the slopes are istics. The result is that, for $F_0 > 1$, the ersect, as shown in Figure 2.6a, because on travels faster. For $F_0 > 1$ the effect he upstream waves over the obstacle to Figure 2.6b. The same processes occur, stream side.

speed being dependent on wave am- spersion, and is illustrated in a simpler f elevation, here simplified to a mono- moving to the left into undisturbed fluid, 1 (2.3.7), which show that the interface in Figure 2.7a. On the other hand, a ing in the same direction and leaving

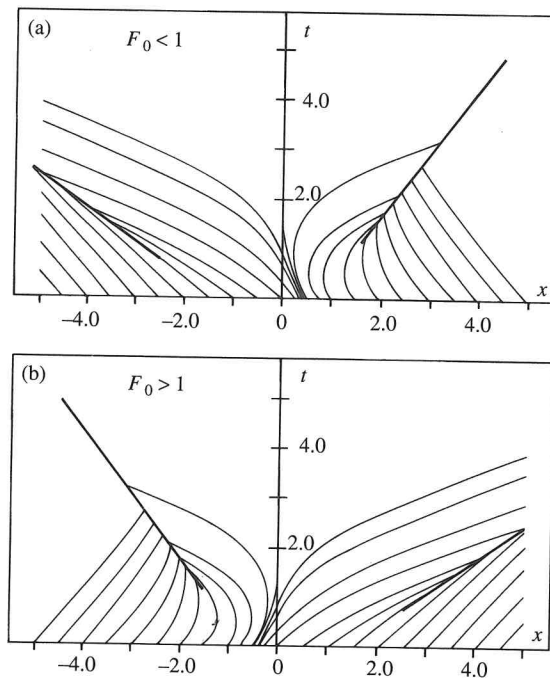


Fig. 2.6. Representative characteristics for the upstream-propagating disturbances for non-linear hydrostatic flow forced by an obstacle impulsively set into motion, when upstream jumps form (cf. Figure 2.1). The obstacle is centred at $x = 0$, and decreases in height to near-zero at $x = \pm 3$. The jumps are denoted by heavy lines. (a) $F_0 < 1$, (b) $F_0 > 1$. (Adapted from Grimshaw & Smyth 1986.)

shallower fluid at rest on the right becomes more spread out, or “rarefied”, with time, as shown in Figure 2.7b. The upstream wave of elevation produced by the starting motion of the obstacle therefore steepens, to the point where the interface becomes vertical, and in principle overturns. Within the framework of the present model, this results in a “hydraulic jump” which may be modelled as a discontinuity, and it is not governed by the above equations *per se*. Hence we must consider its behaviour as an independent entity.

2.3.1 Hydraulic jumps

We consider a simple model of hydraulic jumps based on the principles of mass and momentum conservation, which will be adequate for our present purposes. More detailed properties of jumps will be discussed later in this chapter. We assume that a hydraulic jump may be

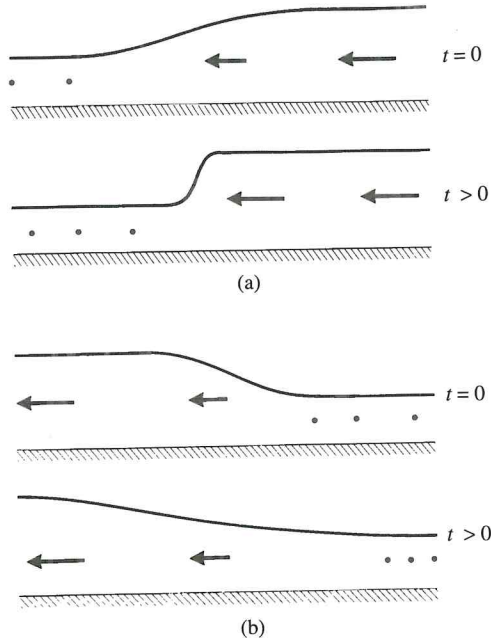


Fig. 2.7. The development of a moving surge according to the hydraulic model. (a) A monotonic increase in depth where the deeper fluid is moving to the left at $t = 0$ into fluid at rest, steepens at subsequent times to form a discontinuity or bore. Arrow length denotes speed of fluid, and dots denote fluid at rest. (b) The reverse situation where the deeper fluid moves away from the depth change, leaving fluid at rest on the right. At later times this disturbance is more spread out, or "rarefied".

regarded as a locally steady and compact region with its own internal dynamics, which may be modelled as a discontinuity between two uniform streams, and that it is produced as a result of wave steepening as just described. We then require equations relating conditions on the upstream and downstream sides of the jump, which must be considered from first principles. At the most fundamental level, we must have conservation of mass and momentum in the region of fluid containing the jump. We take coordinates fixed relative to the jump, and in this frame of reference denote the fluid velocity and depth on the upstream side by u_u and d_u , and on the downstream side by u_d and d_d , as shown in Figure 2.8. Conservation of mass into and out of the jump then gives

$$u_u d_u = u_d d_d = Q, \quad (2.3.8)$$

where Q is the volume flux relative to the jump. Conservation of momentum applied to a vertical column of fluid implies that the

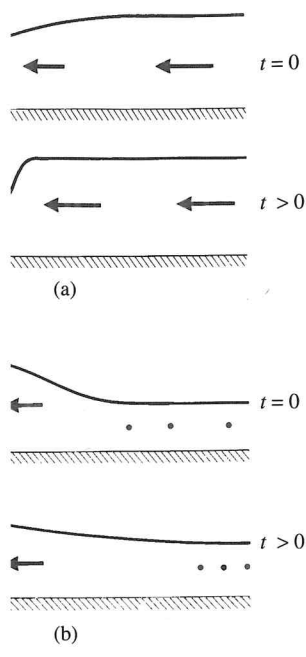


Fig. 2.8. Notation in the frame of a steady hydraulic jump (see text).

vertically integrated form of (2.3.1) applies across the jump, and integrating (2.3.1) vertically and then horizontally gives

$$d_u u_u^2 + \frac{1}{2} g d_u^2 = d_d u_d^2 + \frac{1}{2} g d_d^2. \quad (2.3.9)$$

These two equations completely specify the properties of the jump at this level of approximation, and enable relevant properties to be calculated. One of these is the rate of energy dissipation within the jump. The energy density of a column of fluid is given by

$$E = \frac{1}{2} \rho_0 du^2 + \frac{1}{2} \rho_0 g d^2, \quad (2.3.10)$$

and from (2.3.1, 2.3.2), over level ground the rate of change of energy is given by

$$\frac{\partial E}{\partial t} = - \frac{\partial}{\partial x} \rho_0 \left(\frac{1}{2} d u^3 + g u d^2 \right) = - \frac{\partial}{\partial x} \rho_0 Q R, \quad (2.3.11)$$

where $\rho_0 Q R = \rho_0 d u (u^2/2 + g d)$ may be identified as the *flux* of energy. Note that the flux of energy is not simply given by $u E$, because each fluid column is not independent of the others, and account must be taken of work done by the pressure force that acts between them (see (1.3.3–6)). The rate of energy dissipation within the jump is then given by the differences between the energy fluxes into and out of the jump, namely

$$\frac{dE_J}{dt} = \rho_0 Q (R_u - R_d) = \frac{\rho_0 g Q}{4} \frac{(d_d - d_u)^3}{d_d d_u}, \quad (2.3.12)$$

where E_J denotes the energy of the fluid in a region containing the jump and moving with it. The mechanisms for this energy dissipation depend on the detailed internal dynamics of the jump, and (2.3.12) is effectively a requirement imposed by the external conditions. Note that for the energy dissipation to be positive we must have $d_d > d_u$.

For a jump advancing into water that is at rest, the speed of the jump in this frame, c_J , is given by $u_u = c_J$, and eliminating u_d from (2.3.8, 2.3.9) yields

$$c_J^2 = \frac{g d_d}{2} \left(1 + \frac{d_d}{d_u} \right), \quad (2.3.13)$$

surge according to the hydraulic model. (a) where the deeper fluid is moving to the left at subsequent times to form a discontinuity in the flow field, and dots denote fluid at rest. (b) where the deeper fluid moves away from the depth right. At later times this disturbance is more

compact region with its own internal structure. Modelled as a discontinuity between two regions produced as a result of wave steepening, the structure equations relating conditions on the two sides of the jump, which must be considered at the most fundamental level, we must have the momentum in the region of fluid containing the fixed relative to the jump, and in this region the fluid velocity and depth on the upstream and downstream side by u_d and d_d , as shown in Fig. 2.8. The mass into and out of the jump then gives

$$u_u = u_d d_d = Q, \quad (2.3.8)$$

relative to the jump. Conservation of the total column of fluid implies that the

a speed which is faster than that of linear waves on fluid of depth d_d (where wave speed $c = \sqrt{gd_d}$), because the fluid following the jump is moving in the same direction in this reference frame.

2.3.2 Flow solutions with topography

The steady-state flow solutions may be specified by the two dimensionless parameters F_0 and $H_m = h_m/d_0$, where h_m is the maximum height of the topography. If h_m is sufficiently small the solution is approximately linear, as described by (2.2.5). Here, when $F_0 < 1$ the upstream disturbance escapes from the region of the obstacle, and for $F_0 > 1$, the corresponding wave is advected away downstream. In both cases, we are left with a steady disturbance over the obstacle, where the upstream conditions are unchanged from the initial ones of $u = U$, $d = d_0$. The steady-state forms of (2.3.1, 2.3.2) may be expressed as

$$\frac{d}{dx} \left(\frac{1}{2} u^2 + gd + gh \right) = 0, \quad \frac{d}{dx} (ud) = 0, \quad (2.3.14)$$

which give

$$ud = Q = Ud_0, \quad (2.3.15)$$

and

$$\frac{1}{2} u^2 + gd + gh = \frac{Q^2}{2d^2} + gd + gh = \frac{1}{2} U^2 + gd_0, \quad (2.3.16)$$

which gives $d(x)$ as a function of $h(x)$. This equation may be expressed as

$$\frac{1}{2} \left(\frac{F_0 d_0}{d} \right)^2 + \frac{d}{d_0} + \frac{h}{d_0} = \frac{1}{2} F_0^2 + 1, \quad (2.3.17)$$

and the solutions are qualitatively similar to those obtained from linear theory (2.2.5) and shown in Figure 2.1. The range of applicability of (2.3.16, 2.3.17) is limited, though, and the limit is seen from (2.3.14) which gives

$$\left(\frac{u^2}{gd} - 1 \right) \frac{dd}{dx} = \frac{dh}{dx}. \quad (2.3.18)$$

This implies that at the crest of a single-humped obstacle where dh/dx vanishes, either dd/dx also vanishes or the local Froude number F , defined by $F^2 = u^2/gd$, is unity. Also, when $F = 1$ we must have $dh/dx = 0$. Now in these steady solutions we have $F = F_0$ upstream, and for $F_0 < 1$, F increases over the obstacle as d decreases and u increases with increasing h . But from (2.3.18), F can only equal unity at the crest of the obstacle where h has its maximum value, h_m . Hence

at of linear waves on fluid of depth d_0 , because the fluid following the jump is this reference frame.

solutions with topography

may be specified by the two dimensionless H_m/d_0 , where H_m is the maximum height. For sufficiently small the solution is approximated (2.2.5). Here, when $F_0 < 1$ the upstream region of the obstacle, and for $F_0 > 1$, ejected away downstream. In both cases, disturbance over the obstacle, where the angles from the initial ones of $u = U$, of (2.3.1, 2.3.2) may be expressed as

$$gh \Big) = 0, \quad \frac{d}{dx}(ud) = 0, \quad (2.3.14)$$

$$= Q = Ud_0, \quad (2.3.15)$$

$$\frac{d^2}{dx^2} + gd + gh = \frac{1}{2}U^2 + gd_0, \quad (2.3.16)$$

of $h(x)$. This equation may be expressed

$$\frac{d}{d_0} + \frac{h}{d_0} = \frac{1}{2}F_0^2 + 1, \quad (2.3.17)$$

similar to those obtained from linear theory 2.1. The range of applicability of h , and the limit is seen from (2.3.14)

$$- 1 \Bigg) \frac{dd}{dx} = \frac{dh}{dx}. \quad (2.3.18)$$

a single-humped obstacle where dh/dx vanishes or the local Froude number F , ity. Also, when $F = 1$ we must have only solutions we have $F = F_0$ upstream, over the obstacle as d decreases and u it from (2.3.18), F can only equal unity where h has its maximum value, h_m . Hence

F cannot exceed unity and h therefore has a maximum value. In these solutions the flow is subcritical everywhere. Similarly for $F_0 > 1$, F decreases over the obstacle and the solutions are again limited by $F = 1$ at the crest, so that here the flow is supercritical everywhere. This maximum obstacle height specified by $F = 1$ is a function of the initial Froude number F_0 and is shown in Figures 2.10–12 (see pp. 41–5) as the curve BAE. From the above equations this curve is readily shown to be given by

$$H_m = 1 - \frac{3}{2}F_0^{2/3} + \frac{1}{2}F_0^2. \quad (2.3.19)$$

This is the boundary of the regions of $F_0 - H_m$ space containing solutions of wholly sub- or supercritical flows, with steady upstream flow states unaffected by the obstacle. When H_m exceeds these values the flow is more complicated and, as the above theoretical discussion suggests and laboratory experiments have shown, an upstream hydraulic jump forms on the upstream side, and must be incorporated into the flow solution.

For flow over depressions, where $h < 0$, if $F_0 < 1$ the steady solutions with subcritical flow everywhere apply regardless of the depth of the hole, and the same applies to the solutions with supercritical flow if $F_0 > 1$. These flow states stem from two different solutions to the cubic equation (2.3.17) for d/d_0 , and if F_0 is varied through unity for fixed $H_m (< 0)$, the flow state will jump from one to the other. If $F_0 = 1$, the steady solution is indeterminate, and may take either form. This suggests that this flow is unstable and unsteady, at least for small obstacles, and this property is discussed further in section 2.6. Note that flow over depressions of any size may be either sub- or supercritical. Waterfalls are a limiting case. Flow in a waterfall must be supercritical, and hence the flow approaching it must also be supercritical if the depth decreases monotonically in the direction of flow. Subcritical flow may exist upstream if it is separated from this supercritical downstream state by a sill or obstacle, where a transition from sub- to supercritical flow occurs.

The preceding equations may be used to incorporate an upstream jump into the characteristic solutions specified by (2.3.7). However, a much simpler approach to locally steady flows over topography is to look for solutions that are steady in the vicinity of the obstacle, and assume that an upstream hydraulic jump (moving away from the region) exists *ab initio*. In fact, the region downstream of such a jump must be subcritical in the frame of the obstacle, so that waves may

propagate from the obstacle to the jump and vice versa. As discussed above, a jump imposes its own conditions on the flow. In practice, therefore, when an upstream jump forms, the information is transmitted back to the obstacle and affects the flow there; the consequent change is then transmitted back to the jump, and so on, with decreasing magnitude of effects. An equilibration between the two is therefore set up, and this is manifested in the steady-state solutions. In practice, the jump usually forms over, or very close to, the obstacle anyway.

From (2.3.18), where h_m is sufficiently large for (2.3.17) not to be applicable, we must have $F = 1$ at $h = h_m$. We therefore consider a model of the flow as shown in Figure 2.9a, where axes are taken in the frame of the topography, and for the present we consider only the upstream side. The upstream jump is moving to the left at a speed c_l , whereas the other parts of the flow are steady. We therefore have five

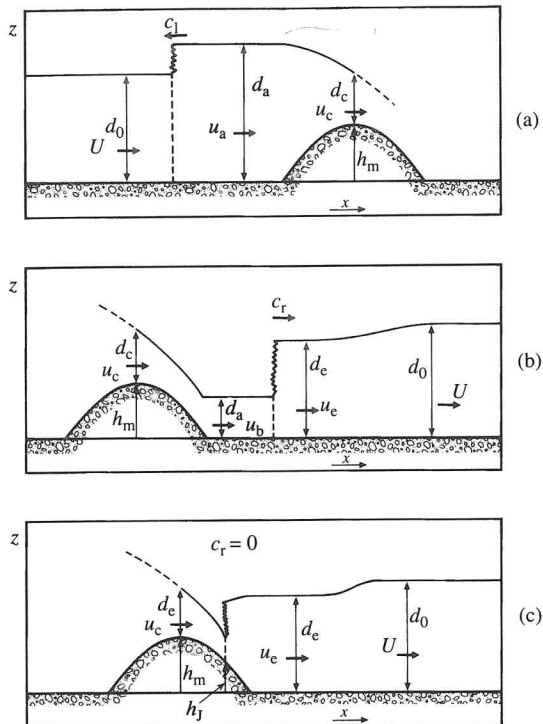


Fig. 2.9. Definition sketches for notation for flow over a long obstacle. (a) Upstream flow with a hydraulic jump; (b) downstream flow with a moving hydraulic jump and rarefaction wave; (c) downstream flow with a stationary hydraulic jump and rarefaction wave.

the jump and vice versa. As discussed in conditions on the flow. In practice, jump forms, the information is transmitted affects the flow there; the consequent to the jump, and so on, with decreasing unbalance between the two is therefore the steady-state solutions. In practice, very close to, the obstacle anyway. sufficiently large for (2.3.17) not to be 1 at $h = h_m$. We therefore consider a figure 2.9a, where axes are taken in the for the present we consider only the mp is moving to the left at a speed c_1 , low are steady. We therefore have five

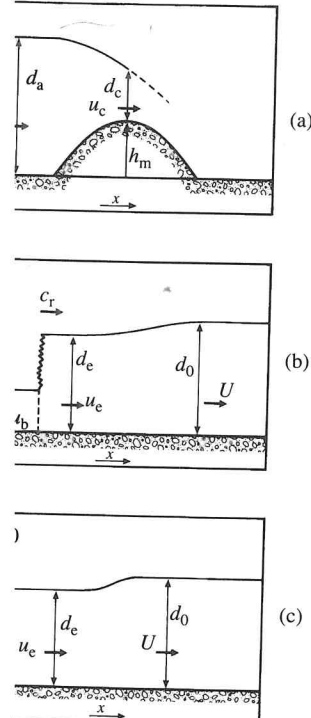


Fig. 2.9. Schematic diagrams of flow over a long obstacle. (a) Upstream flow with a moving jump; (b) downstream flow with a moving jump; (c) downstream flow with a stationary jump.

unknown variables (c_1 , u_a , d_a , u_c and d_c), to be determined by the five equations

$$(U + c_1)d_0 = (u_a + c_1)d_a, \quad (2.3.20)$$

$$u_a d_a = u_c d_c, \quad (2.3.21)$$

$$(U + c_1)^2 = \frac{gd_a}{2} \left(1 + \frac{d_a}{d_0}\right), \quad (2.3.22)$$

$$\frac{1}{2}u_a^2 + gd_a = \frac{1}{2}u_c^2 + g(d_c + h_m), \quad (2.3.23)$$

$$u_c^2 = gd_c. \quad (2.3.24)$$

Here the first two equations come from mass conservation, the third from the jump speed expression (2.3.13), the fourth from the Bernoulli equation (2.3.14, 2.3.15), and the fifth from the critical condition at $h = h_m$. The solution of these equations yields results as shown in Figure 2.10 for the upstream jump speed and its elevation, rendered dimensionless by

$$C_1 = \frac{c_1}{\sqrt{gd_0}}, \quad D_a = \frac{d_a}{d_0}. \quad (2.3.25)$$

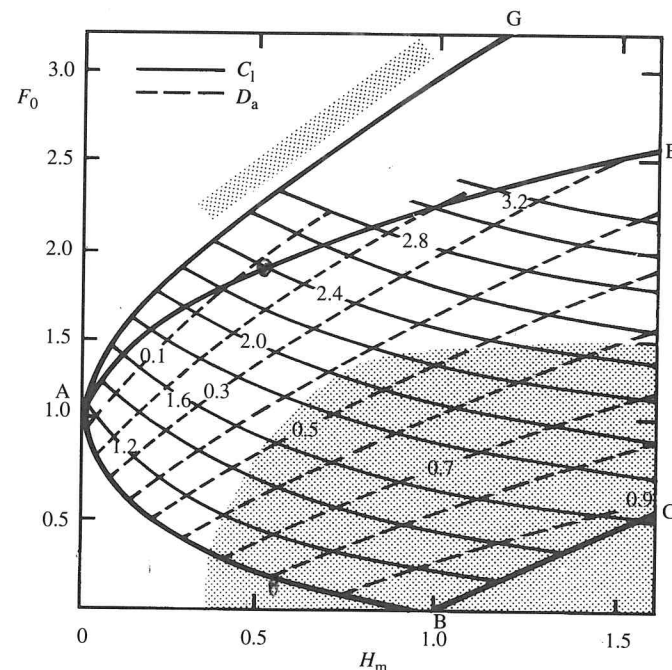


Fig. 2.10. Values for upstream jump speed $C_1 = c_1/\sqrt{gd_0}$ and jump amplitude ($D_a = d_a/d_0$) as functions of F_0 and H_m , from the hydraulic model. The shaded regions denote the parameter ranges covered in Long's (1970) experiments.

Here, curves of constant values of C_1 , D_a are shown in terms of the two fundamental dimensionless parameters of the system, F_0 and H_m . Long (1970, 1972) has made comparisons with laboratory experiments in the regions shown shaded in Figure 2.10, with satisfactory agreement. We note from Figure 2.10 the curious result that solutions to (2.3.20–24) are not confined to the right of the curve BAE, but extend to the curve AG when $F_0 > 1$. AG is determined by the criterion $c_1 = 0$, and may be shown to have the equation

$$H_m = \frac{(8F_0^2 + 1)^{3/2} + 1}{16F_0^2} - \frac{1}{4} - \frac{3}{2}F_0^{2/3}. \quad (2.3.26)$$

Near $F_0 = 1$, $H_m = 0$, the perturbation to the undisturbed flow in the solutions to (2.3.20–24) grows as $H_m^{1/2}$, rather than H_m . As H_m increases, the value of $u_a d_a$ in these solutions progressively decreases, and reaches zero at the curve BC, which is given by

$$F_0 = (H_m - 1) \left(\frac{1 + H_m}{2H_m} \right)^{1/2}. \quad (2.3.27)$$

To the right of this curve, there is no flow over the obstacle, as the latter is high enough to block the flow completely. On this boundary $D_a = H_m$, and to the right of it $D_a < H_m$; further increases in H_m with F_0 constant cannot change the upstream flow properties. The flow states pertaining to these various regions of the $F_0 - H_m$ diagram are shown in Figure 2.11. When $F_0 = 4.47$, curve BC intersects AE at a point (not shown) denoted by K, and BC continues and asymptotes to a straight line that is parallel to AG. In the region CKE, in which $F_0 > 4.47$, $H_m > 6.90$, the steady flow is either supercritical everywhere, or totally blocked.

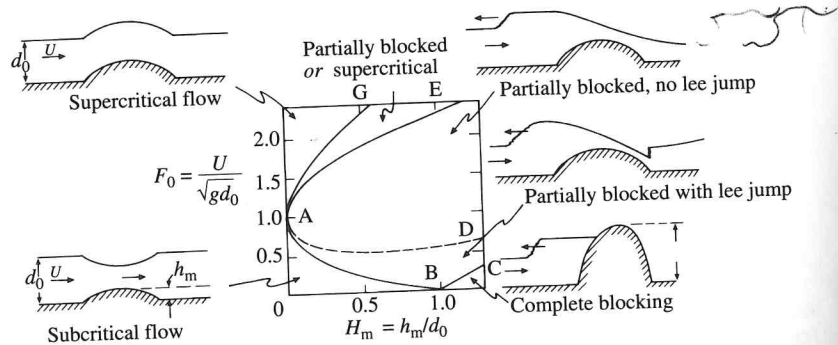


Fig. 2.11. Flow regimes on the $F_0 - H_m$ diagram for hydrostatic single-layer flow over an obstacle.

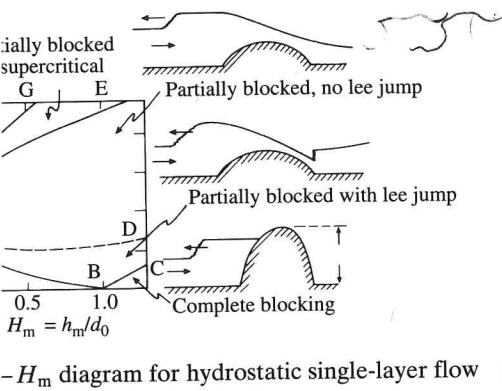
as of C_1 , D_a are shown in terms of the parameters of the system, F_0 and H_m . Comparisons with laboratory experiments in Figure 2.10, with satisfactory agreement, show the curious result that solutions to the right of the curve BAE, but extend beyond AG. AG is determined by the criterion involving the equation

$$\frac{1)^{3/2} + 1}{6F_0^2} - \frac{1}{4} - \frac{3}{2} F_0^{2/3}. \quad (2.3.26)$$

turbation to the undisturbed flow in the vs as $H_m^{1/2}$, rather than H_m . As H_m these solutions progressively decreases, BC, which is given by

$$-1\left(\frac{1+H_m}{2H_m}\right)^{1/2}. \quad (2.3.27)$$

ere is no flow over the obstacle, as the the flow completely. On this boundary that $D_a < H_m$; further increases in H_m with he upstream flow properties. The flow regions of the $F_0 - H_m$ diagram are $F_0 = 4.47$, curve BC intersects AE at a K, and BC continues and asymptotes to l to AG. In the region CKE, in which ready flow is either supercritical every-



$-H_m$ diagram for hydrostatic single-layer flow

Within region EAG, the flow may be either supercritical, as in the region to the left of AG, or controlled by a critical condition at the crest with an upstream jump, as in the region to the right of AE. Although the governing equations have been known for a hundred years or more, the presence of these two different flow states in region EAG is a relatively recent discovery. [Curve BAG was described by Long (1954, 1970), curve BAE by Houghton & Kasahara (1968), and region EAG by Baines & Davies (1980).] The presence of these two states implies that the state obtained in practice depends on the initial conditions. It also implies that there is *hysteresis* in the system. If, for example, one starts with a steady supercritical state in EAG and then slowly decreases F_0 so that the flow evolves quasistatically through a succession of steady states, on reaching AE the flow suddenly changes from supercritical flow to the critically controlled state with the upstream jump. If one then reverses the process and increases F_0 , this new state persists until curve AG is reached, where the flow makes a sudden transition back to the supercritical state. Similar transitions occur if F_0 is held constant and H_m is increased and decreased. This hysteresis has been verified numerically by Pratt (1983), and it may be readily demonstrated in a hydraulic laboratory.

When the flow is critically controlled at the obstacle crest, the downstream flow may have one of the two forms shown in Figure 2.9b and c (Houghton & Kasahara 1968). Flow on the lee side is supercritical (i.e. $F > 1$) and is followed by a hydraulic jump that may be swept downstream as in Figure 2.9b, or situated over the topography as in Figure 2.9c. However, these structures alone do not permit the downstream flow to be equated to the initial flow state. This connection may be made by adding a time-dependent downstream propagating wave. This is a rarefaction wave propagating into fluid at rest on the one family of characteristics only, and as for (2.3.6), (2.3.4, 2.3.5) give

$$u_e - 2\sqrt{gd_e} = U - 2\sqrt{gd_0}. \quad (2.3.28)$$

For the configuration and notation of Figure 2.9b, we again have five undetermined variables, and the five equations

$$u_c d_c = u_b d_b, \quad (2.3.29)$$

$$\frac{1}{2} u_c^2 + g(d_c + h_m) = \frac{1}{2} u_b^2 + g d_b, \quad (2.3.30)$$

$$(u_b + c_r)^2 = \frac{g d_e}{2} \left(1 + \frac{d_e}{d_b}\right), \quad (2.3.31)$$

$$(u_b + c_r)d_b = (u_e + c_r)d_e, \quad (2.3.32)$$

and (2.3.28), which enable u_b , d_b , u_e , d_e and c_r to be determined. Here (2.3.29, 2.3.32) come from mass conservation, (2.3.30) from the Bernoulli equation over the obstacle, and (2.3.31) from the jump speed relation (2.3.13). These equations apply above the dashed line AD in Figure 2.11, where $c_r = 0$ on this line. Below AD the configuration of Figure 2.9c is applicable, with a stationary jump over the lee side of the obstacle. Here we have seven unknowns: u_- , d_- , and u_+ , d_+ , which are the flow variables immediately upstream and downstream of the jump respectively, u_e , d_e , and h_J , the height of the topography at the location of the jump. The equations are

$$u_c d_c = u_- d_- = u_+ d_+ = u_e d_e, \quad (2.3.33)$$

$$u_-^2 = \frac{g d_+}{2} \left(1 + \frac{d_+}{d_-} \right), \quad (2.3.34)$$

$$\frac{1}{2} u_c^2 + g(d_c + h_m) = \frac{1}{2} u_-^2 + g(d_- + h_J), \quad (2.3.35)$$

$$\frac{1}{2} u_+^2 + g(d_+ + h_J) = \frac{1}{2} u_e^2 + g d_e, \quad (2.3.36)$$

and (2.3.28), from which the details of the flow may be found. Respectively these equations come from conservation of mass, the condition for a stationary jump ($c_r = 0$), and the Bernoulli equations over the obstacle. Curves showing the values of c_r (above AD) and h_J (below AD) are shown in Figure 2.12.

In the blocked flow region to the right of curve BC in Figure 2.11, the downstream jump disappears and the downstream flow is completely governed by the condition (2.3.28) with $u_e = 0$. This gives

$$\frac{d_e}{d_0} = \left(1 - \frac{F_0}{2} \right)^2, \quad (2.3.37)$$

so that d_e decreases from $d_0/4$ to zero as F_0 increases from 1 to 2, and must vanish for $F_0 \geq 2$ where the fluid “dries out” on the lee side of the obstacle.

In the region enclosed by EADC (or GADC) of Figure 2.11, the drag force on the obstacle is

$$F_D = \int p \frac{dh}{dx} dx = \frac{\rho g}{2} \frac{(d_a - d_b)^3}{d_a + d_b}, \quad (2.3.38)$$

where $p = \rho g d$ is the pressure on the topographic surface.

2.3.3 Flow through variable cross-sections and lateral contractions

Single-layer flow through a channel whose cross-section varies on length-scales that are long compared with the channel width and depth,